Preferred sensor sites for surface EMG signal decomposition

2012 Physiol. Meas. 33 195

(http://iopscience.iop.org/0967-3334/33/2/195)

IOP PUBLISHING PHYSIOLOGICAL MEASUREMENT

Physiol. Meas. **33** (2012) 195–206 doi:10.1088/0967-3334/33/2/195

Preferred sensor sites for surface EMG signal decomposition

Farah Zaheer[1,2,5], **Serge H Roy**[1,2] **and Carlo J De Luca**[1,3,4]

[1] NeuroMuscular Research Center, Boston University, Boston, MA 02215, USA
[2] Sargent College of Health and Rehabilitation Sciences, Boston University, Boston, MA 02215, USA
[3] Department of Biomedical Engineering, Boston University, Boston, MA 02215, USA
[4] Department of Electrical and Computer Engineering, Boston University, Boston, MA 02215, USA

E-mail: farahz@bu.edu

Received 21 July 2011, accepted for publication 28 November 2011
Published 20 January 2012
Online at stacks.iop.org/PM/33/195

Abstract

Technologies for decomposing the electromyographic (EMG) signal into its constituent motor unit action potential trains have become more practical by the advent of a non-invasive methodology using surface EMG (sEMG) sensors placed on the skin above the muscle of interest (De Luca *et al* 2006 *J. Neurophysiol.* **96** 1646–57 and Nawab *et al* 2010 *Clin. Neurophysiol.* **121** 1602–15). This advancement has widespread appeal among researchers and clinicians because of the ease of use, reduced risk of infection, and the greater number of motor unit action potential trains obtained compared to needle sensor techniques. In this study we investigated the influence of the sensor site on the number of identified motor unit action potential trains in six lower limb muscles and one upper limb muscle with the intent of locating preferred sensor sites that provided the greatest number of decomposed motor unit action potential trains, or motor unit yield. Sensor sites rendered varying motor unit yields throughout the surface of a muscle. The preferred sites were located between the center and the tendinous areas of the muscle. The motor unit yield was positively correlated with the signal-to-noise ratio of the detected sEMG. The signal-to-noise ratio was inversely related to the thickness of the tissue between the sensor and the muscle fibers. A signal-to-noise ratio of 3 was found to be the minimum required to obtain a reliable motor unit yield.

Keywords: sEMG signal decomposition, sEMG sensor, motor units, motor unit action potential train

(Some figures may appear in colour only in the online journal)

[5] Author to whom any correspondence should be addressed.

1. Introduction

Over the past several decades, methodologies for decomposing the electromyographic (EMG) signal into its constituent motor unit action potential trains (MUAPTs) have predominantly relied upon the use of a needle sensor inserted into the muscle of interest to record the EMG signals (LeFever and De Luca 1982, Nawab *et al* 2008). Drawbacks of this technology, related to the invasiveness of the procedures and limited motor unit (MU) yields, have prompted a number of researchers to seek a non-invasive alternative (Holobar *et al* 2009, Merletti *et al* 2009, Gazzoni *et al* 2004). These prior attempts have been minimally effective toward a non-invasive surface EMG solution because of relatively low motor unit yields (3–6 MUs) and low force level contractions (∼5–9% of maximal voluntary contraction, MVC). However, recent developments by De Luca *et al* (2006) and Nawab *et al* (2010) have advanced the state of the art to achieve a non-invasive technology (figure 1) that produces high MU yields (typically 30–40) with high accuracies (>95%) over the full force range (0–100% MVC) from a wide variety of superficial muscles.

The algorithm identifies the individual action potentials within the sEMG signals and allocates them to individual MUAPTs. This operation is presently done with a measured accuracy averaging 95.2% and at times reaching 100% (for details see Nawab *et al* (2010), and the appendix of De Luca and Hostage (2010)). Presently, the technology is able to identify the firings of 30–40 MUs (occasionally surpassing 50) from sEMG signals obtained during isometric constant-force contractions. An example of the decomposed sEMG signal is presented in figure 2. The top panel shows one of the four channels of the sEMG signal along with the firing instances of 34 MUs. An expanded view of 6 MUAPTs (# 26–31) is shown on the right side. The action potential shape of each of the MUs is displayed near the left axis. The dark line represents the force produced by the subject.

Currently there are no guidelines for locating the surface sensor specifically for motor unit decomposition studies. However, we have observed that the site of the sensor on the muscle surface influences the number of MUAPTs that are identified by the decomposition algorithm. The present study was undertaken to systematically quantify these observations. Furthermore, we investigated whether the skinfold thickness, and its relationship to signal quality, influences the MU yield.

2. Methods

2.1. Subjects

Four neurologically healthy subjects, aged 18–22 years (mean = 21, SD = ±1.89), volunteered for the study. The body mass index for the subjects ranged from 21.9 to 24 (mean = 22.8); all were within normal limits (Cole 1991). All subjects read and signed an informed consent form approved by the Institutional Review Board of Boston University prior to their participation.

2.2. Muscles

The following skeletal muscles in each subject were tested: *Biceps Brachii* (BB), *Vastus Lateralis* (VL), *Rectus Femoris* (RF), Hamstrings (HS) group, *Gastrocnemius* (GS), *Soleus* (SL) and *Tibialis Anterior* (TA) muscles. No distinction was made between the *Semitendinosis, Semimembranosis* and the *Biceps Femoris* muscle compartments of the HS group. The BB, GS and HS muscles were considered as individual medial and lateral sections. The muscles

Figure 1. The sEMG sensor, the signal acquisition and amplification unit and a PC loaded with the decomposition algorithm are shown. The pins on the sEMG sensor are 1.25 mm long and approximately 0.57 mm in diameter; four of which are located at the corner of a 5 mm^2, and one in the center of the square.

were selected because they provide examples of superficial limb muscles with a relatively large area for sensor placement, and because they are overlaid with varying amounts of fatty tissue.

2.3. Sensor sites

In previous pilot observations in our laboratory, a substantial region covering the entire muscle belly had been sampled with the surface sensor electrode for each muscle. The decomposition results from these observations guided the selection of the final candidate sites to be sampled systematically in the present study. The dominant factor in the site selection for each muscle was to focus primarily on those areas that had the relatively richer MU yields. The sensor sites were furthermore chosen to attain a balance between the available area of the muscle belly, the size of the surface sensor itself and the limitation on the total number of sensor sites that could be assayed without introducing fatigue. Therefore, the total number of sites usually ranged from 10 to 12 per muscle.

A rectangular template whose length approximated the borders of the myo-tendinous regions of the muscle, and whose width approximated the lateral margins of the muscle belly (figure 3) was drawn on each muscle. The location of the tendinous junction and the width of the muscle were confirmed by palpation. For the SL muscle, the surface area available for testing was in the form of a V. The sensors for this muscle were placed linearly along the exposed surfaces directly beneath the gastrocnemius muscle.

2.4. EMG signal acquisition

The skin surface was debrided using multiple applications of a hypoallergenic tape and was then wiped with an isopropanol alcohol prep pad. This procedure improved the quality of electrical contact between the pins of the sensor and the skin. The sensor was attached to the skin at a designated sensor site. A 4 cm diameter adhesive gel reference electrode (Dermatrode®) was placed on a bony region on either the elbow or the kneecap. The procedure for acquiring the signal is described by De Luca *et al* (2006). Briefly, sEMG signals from the four differential pairs of the sensor array were band-pass filtered at 20 Hz (12 dB/octave) to 1750 Hz (24 dB/octave) and digitized with 16-bit resolution at a sampling rate of 20 kHz. The force data were band-pass filtered from DC-550 Hz and sampled at the same rate as the sEMG signal.

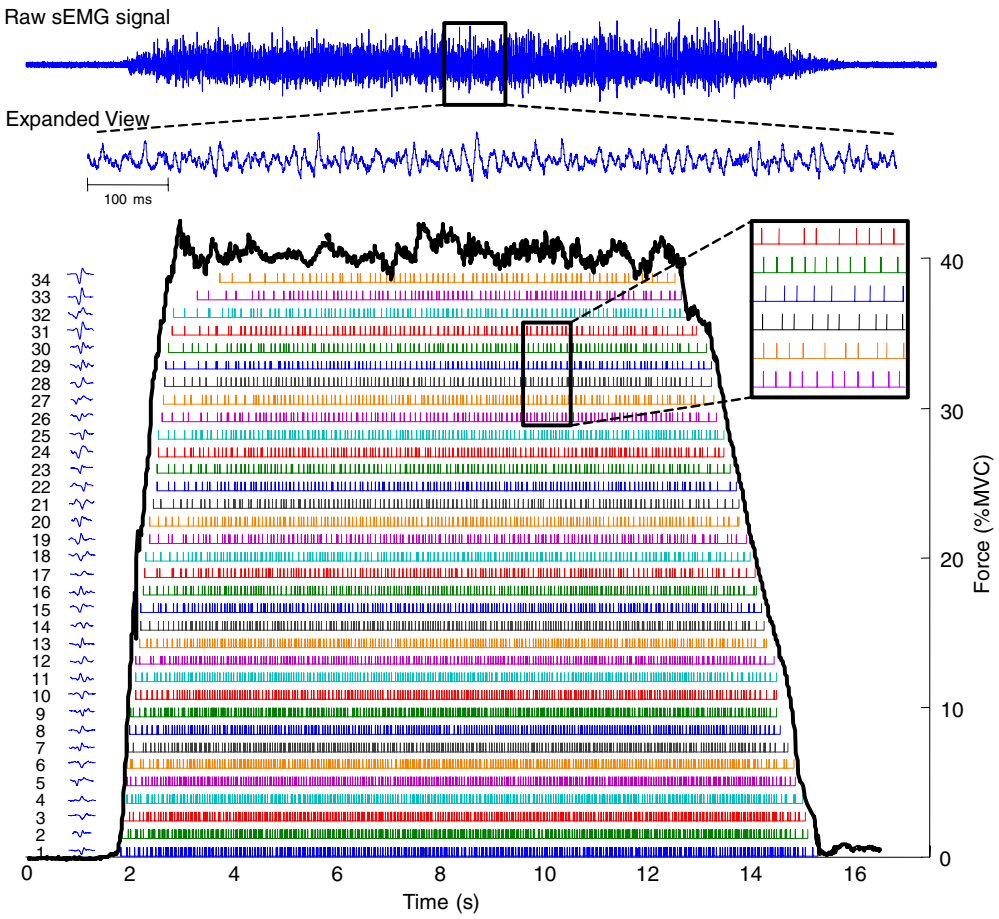

Figure 2. The raw sEMG signal on the top represents one of the four channels of differentially detected signal from a pair of pins on the sensor. Below the signal is an expanded epoch to show the complexity of the signal. The signal was acquired during an isometric constant force contraction at 40% MVC from the HS muscle. The force produced by the muscle is shown as a dark black line. The bars represent the firing times of the action potentials from 34 motor units identified by the decomposition algorithm. The frame on the left shows a time scale expanded view of the firing instances. The waveforms on the left represent the action potentials from each of the motor units.

2.5. Test procedure

A protocol was designed to acquire sEMG signals from each of the sensor sites according to a randomized sampling procedure, in order to negate the possible influence of muscle fatigue on MU activity. The subject was positioned in a custom chair (Adam and De Luca 2003) for testing the lower limb muscles. The lower limb was fixed so that designated isometric knee or ankle forces could be maintained against a load cell, either during joint extension (such as for testing the VL, RF and TA muscles) or flexion (such as for testing the HS, GS, and SL muscles). The hip and ankle joints were fixed at 90° while the knee angle was varied depending on the test muscle to be sampled (*120*° for the RF, VL, TA and SL muscles; *110*° for the HS muscle; and *180*° for the GS muscle). For the BB muscle, an adjustable strap attached to a load cell was held by the subject in the supinated hand position, with the length of the strap adjusted to maintain 90° of elbow flexion.

In order to compare force levels across subjects, the MVC was obtained for each subject by requesting that they contract the test muscle as forcefully as possible. These contractions were repeated three times for each muscle, with a 3 min rest between the contractions. The greatest value was taken as the MVC level. All subsequent contractions for each subject were referenced to this value. Executing an MVC is an unfamiliar task; hence the subjects were required to practice the MVC and force trajectory tracking tasks on a separate day prior to the data collection experiments.

The sensor was placed on one of the candidate sensor sites of the muscle grid. The subjects were asked to track a trapezoidal force trajectory that consisted of an initial 10% MVC/s ramp to a 40% MVC plateau that was sustained for 10 s followed by a downward ramp at 10% MVC/s. The subjects used visual force feedback from a display monitor to comply with the task. A 40% MVC level was specified because it provided substantial recruitment of MUs without fatiguing the subject. A sample force trajectory may be seen in figure 2. The sensor was moved to another site on the muscle template and the protocol was repeated. This process was repeated until all the candidate sensor sites on the muscle had been sampled. At the end of the experiments, the tissue thickness at each of the sensor sites was measured according to the procedure described by Edwards (1954). The skin and subcutaneous tissue at each test site was lifted by pinching it with the thumb and the index finger and measuring the thickness using a spring-loaded caliper (*SAEHAN* Medical Skinfold Caliper Model # SH5020) positioned at the center of the folded skin.

2.6. Data analysis

Task compliance for the force trajectory was assessed by calculating the root-mean-squared value of the difference between the force produced by the subject and the target force level during the plateau region. This error amplitude was expressed as a percentage of the MVC level for normalization across subjects. A maximum deviation of $\pm 1\%$ MVC was allowed. Only data from trials that met the task compliance requirements were subsequently analyzed. A total of 304 files were decomposed using the algorithm described by Nawab *et al* (2010). A sample decomposition result is shown in figure 2, where the firings of 34 distinct MUs were identified. This is the MU yield which was obtained for each sensor site of each muscle. In order to determine the degree of MU yield throughout the various sensor sites within each muscle, the MU yields were normalized with respect to the greatest MU yield from all the contractions of that test muscle, and then averaged across all subjects. Hence, the normalized MU yields ranged from 0 to 1 in all muscles. The signal-to-noise ratio (SNR) at each site was computed as the ratio of the root-mean-squared sEMG signal in a 3 s epoch from the constant force region to that of a 3 s signal from the baseline at 0% MVC. An epoch of 3 s provides an adequate window of time because both the sEMG signal and the baseline noise are stationary signals.

3. Results

A total of 4120 MUAPTs were obtained from 304 contractions from seven muscles derived from $n = 4$ subjects.

3.1. Preferred sensor sites

Table 1 reports the range of MU yields for each subject by muscle. The MU yield from the various muscles ranged anywhere from 3 to 40 with a particularly restricted range obtained in

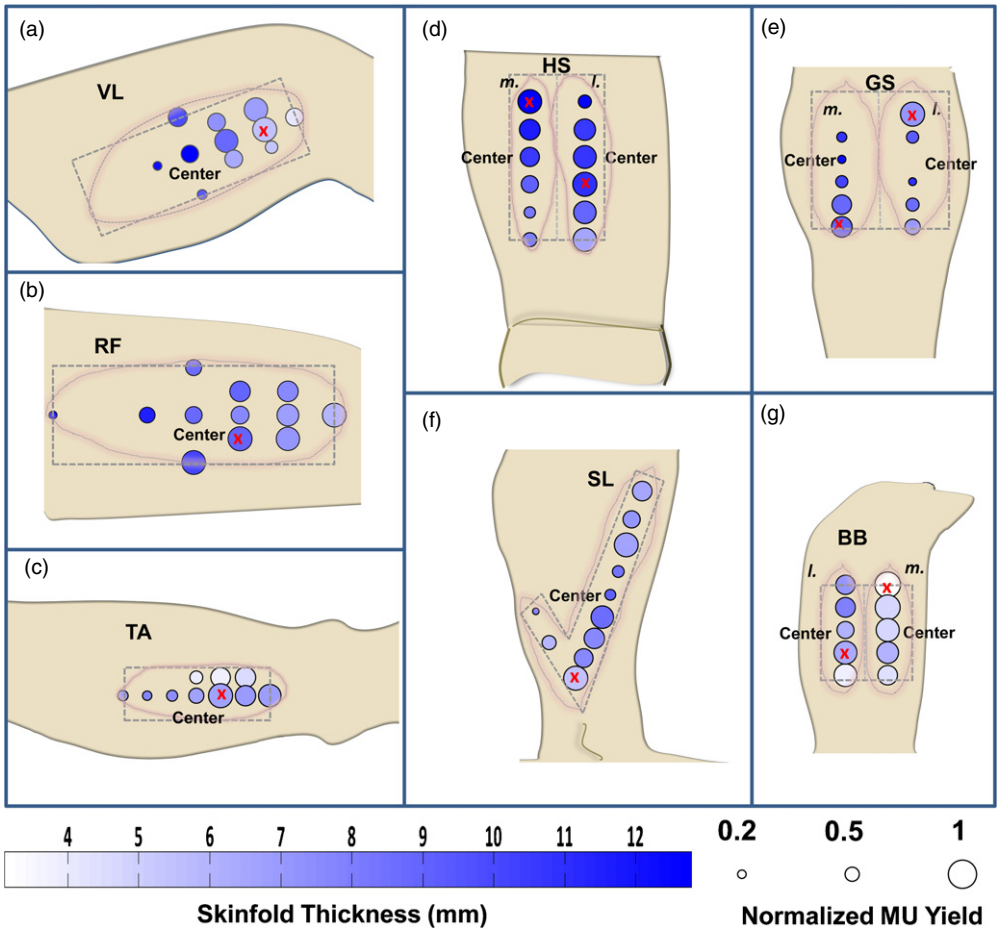

Figure 3. The seven tested muscles are topographically mapped by the normalized MU yield per sensor site (see section 3.1) with increasing circle sizes reflecting greater yields indicated by the scale below. The average skinfold thickness is indicated by the hue of the color as indicated in the scale below. The values for each muscle are as follows: (a) Vastus lateralis: The normalized MU yield ranges from 0.3 to 0.9 and the skinfold ranges from 4 to 12.6 mm. (b) Rectus femoris: The normalized MU yield ranges from 0.3 to 0.8 and the skinfold ranges from 5.9 to 12.4 mm. (c) Tibialis anterior: The normalized MU yield ranges from 0.4 to 1 and the skinfold ranges from 3.3 to 6.7 mm. (d) Hamstrings medial: The normalized MU yield ranges from 0.4 to 0.9 and the skinfold ranges from 7.8 to 11.5 mm. Hamstrings lateral: The normalized MU yield ranges from 0.5 to 0.9 and the skinfold ranges from 6.4 to 12.5 mm. (e) Gastrocnemius medial: The normalized MU yield ranges from 0.3 to 0.9 and the skinfold ranges from 6 to 12.6 mm. Gastrocnemius lateral: The normalized MU yield ranges from 0.3 to 1 and the skinfold ranges from 6 to 12 mm. (f) Soleus: The normalized MU yield ranges from 0.2 to 0.9 and the skinfold ranges from 5.4 to 9 mm. (g) Biceps brachii medial: The normalized MU yield ranges from 0.7 to 1 and the skinfold ranges from 3.1 to 6.7 mm. Biceps brachii lateral: The normalized MU yield ranges from 0.6 to 0.9 and the skinfold ranges from 3.3 to 8.5 mm.

the gastrocnemius muscles. The values of the normalized MU yields for each site on all the muscles are plotted in figure 3. The radius of the circle on each site represents the normalized MU yield, with values ranging from 0.2 to 1. The shade of color in the circle is proportional to the average skinfold thickness of that site, with darker shades representing greater skinfold thicknesses. The skinfold color scale ranges from 3.1 to 12.6 mm.

Table 1. The MU range in each muscle for each subject is reported.

Muscle	Subj 1	Subj 2	Subj 3	Subj 4
Vastus lateralis	7–11	15–26	3–30	5–25
Rectus femoris	3–15	6–20	7–30	10–39
Tibialis anterior	11–32	6–28	8–35	10–35
Soleus	3–22	3–14	5–25	6–17
Hamstrings medial	14–34	3–31	14–28	14–29
Hamstrings lateralis	20–25	17–28	5–28	5–15
Gastrocnemius medial	5–6	3–16	3–15	5–23
Gastrocnemius lateral	5–12	3–9	5–15	3–18
Biceps brachii medial	18–40	12–28	25–35	14–33
Biceps brachii lateral	17–34	3–24	19–34	4–27

Table 2. Landmarks for the preferred sensor sites are referenced from the center of the muscle belly. (In the SL muscle, due to the nonrectangular asymmetrical V shape, the sensor site labeled as 'center' was used as the origin.)

Muscle	Preferred site
Vastus lateralis	2/3 Distal from the center
Rectus femoris	1/3 Distal-lateral from the center
Tibialis anterior	1/3 Distal from the center
Soleus	Distal end from the center
Hamstrings medial	2/3 Proximal from the center
Hamstrings lateralis	1/3 Distal from the center
Gastrocnemius medial	Distal end from the center
Gastrocnemius lateral	2/3 Proximal from the center
Biceps brachii medial	Proximal end from the center
Biceps brachii lateralis	1/2 Distal from the center

The normalized MU yield was site dependent for all the muscles and the range was higher for the VL, GS (both lateral and medial heads), SL and TA muscles compared to the HS, RF and BB muscles. The HS, RF and BB muscles had several sensor sites with similar normalized MU yield. Sites corresponding to the highest normalized MU yield in each muscle are indicated with an 'X' symbol and are referred to as preferred sensor sites (table 2). For example, in the VL muscle (figure 3(a)), the preferred site was identified at approximately two-thirds the distance from the center of the muscle belly toward the distal tendon. The MU yield ranged from 3 to 30 across all subjects in this muscle. The highest yielding sensor sites for the RF and TA muscles were also located in the distal portions of the muscle, as shown in figures 3(b) and (c). In the GS muscle, there was a contrasting distribution of normalized MU yield for the two separate heads. The medial GS had its preferred site in the most distal portion of the muscle, whereas for the lateral head it was near the proximal end (figure 3(e)). MU yield was also studied separately for each of the two heads of the BB and the HS muscles. For the medial heads of these muscles, the preferred site was located in the proximal portions of the muscle, whereas for the lateral head of the BB and HS it was distally located at 1/2 and 1/3 of the way from the center of the muscle respectively (figures 3(d) and (g)). The preferred site for the SL muscle was also located in the distal portion of the muscle as illustrated in figure 3(f). A few muscles such as the VL, RF, medial BB and lateral HS muscles in fact had several adjacent sensor sites with similar normalized MU yields constituting a preferred region as opposed to just one site.

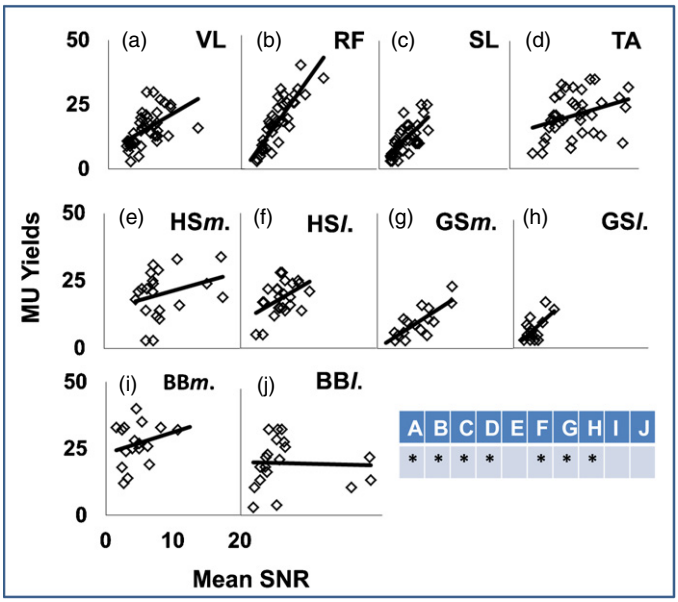

Figure 4. The regressions of MU yields against the mean SNR of each muscle are plotted in each subpanel. The table indicates with an asterisk (*) the correlations that were found to be significant.

Table 3. The correlations (R^2) of the MU yield/mean SNR, mean SNR/skinfold as well as MU yield/skinfold in each muscle are presented. An asterisk (*) indicates those correlations that are statistically significant at $p < 0.05$.

Muscle	MU yield/SNR	SNR/skinfold	MU yield/skinfold
Vastus lateralis	$r^2 = 0.27^*$	$r^2 = 0.25^*$	$r^2 = 0.13^*$
Rectus femoris	$r^2 = 0.73^*$	$r^2 = 0.16^*$	$r^2 = 0.11^*$
Tibialis anterior	$r^2 = 0.11^*$	$r^2 = 0.28^*$	$r^2 = 0.01$
Soleus	$r^2 = 0.48^*$	$r^2 = 0.25^*$	$r^2 = 0.03$
Hamstrings medial	$r^2 = 0.09$	$r^2 = 0$	$r^2 = 0.58^*$
Hamstrings lateralis	$r^2 = 0.22^*$	$r^2 = 0.33^*$	$r^2 = 0.01$
Gastrocnemius medial	$r^2 = 0.61^*$	$r^2 = 0.08$	$r^2 = 0.31^*$
Gastrocnemius lateral	$r^2 = 0.38^*$	$r^2 = 0.06$	$r^2 = 0.07$
Biceps brachii medial	$r^2 = 0.06$	$r^2 = 0.17$	$r^2 = 0.03$
Biceps brachii lateral	$r^2 = 0$	$r^2 = 0.25^*$	$r^2 = 0.04$

3.2. MU yield and SNR

MU yield for each site was positively correlated with the SNR of the sEMG signal for most of the muscles. In particular, for medial and lateral GS, VL, RF, SL, TA and lateral HS, MU yields were significantly correlated with SNR (R^2 range 0.11–0.73; p <0.05). For the medial HS and BB muscles the positive relationship was not found to be significant. These results are displayed in figure 4 with R^2 values presented in table 3.

3.3. SNR and skinfold

The SNR of the sEMG signal was negatively correlated with the skinfold thickness for some of the muscles. In particular, the VL, TA, RF, SL and lateral BB and lateral HS muscles have significant correlations (R^2 range 0.16–0.33; $p < 0.05$). The GS (both lateral and medial

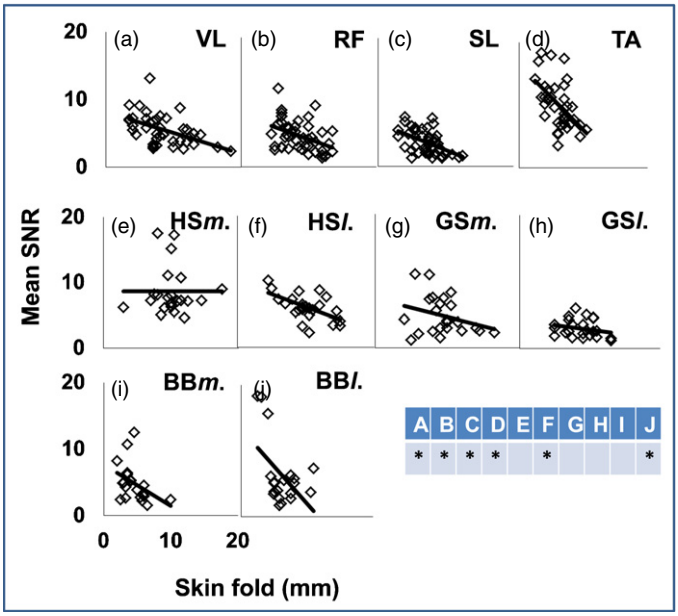

Figure 5. The regressions of the mean SNR against the skinfold thickness. Each panel contains the data from one of the tested muscles. The table indicates the significant correlations with the asterisk (*) at $p < 0.05$. See table 3 for statistics.

heads), the medial BB and medial HS muscles were also negatively correlated with skinfold thickness, but the trend did not reach statistical significance. These results are displayed and tabulated in figure 5 and table 3.

3.4. MU yield and skinfold

The MU yield per site had only moderate negative correlations with skinfold thickness for some of the muscles tested, as shown in figure 6 and table 3. The MU yield versus skinfold relationship is significant ($p < 0.05$) for the VL, RF, and medial GS muscles with R^2 ranging between 0.1 and 0.31 while not reaching statistical significance in the SL, TA, medial BB and lateral GS muscles. In the VL and RF muscles localized high yield sensor sites were mostly found in areas with reduced skinfold thickness. This association is visually depicted by the coloring scheme in figure 3. For example, in the VL muscle, the areas with reduced skinfold thickness, denoted by the lighter circle colors, were associated with higher decomposition yields characterized by the larger circle areas. Similarly in the proximal regions for this muscle where the skinfold thickness is considerably greater, the circle sizes are smaller and they are darker in color. However, this association is not present in the HS muscle. In fact, the medial HS muscle has a significant positive correlation between skinfold thickness and MU yield. The slightly positive trend also obtained in the lateral HS and lateral BB muscles was however not significant ($p < 0.05$).

4. Discussion

Our results confirm that there are preferred regions on the surface of the muscle which provide richer MU yields. The preferred region was located either in the proximal or the distal

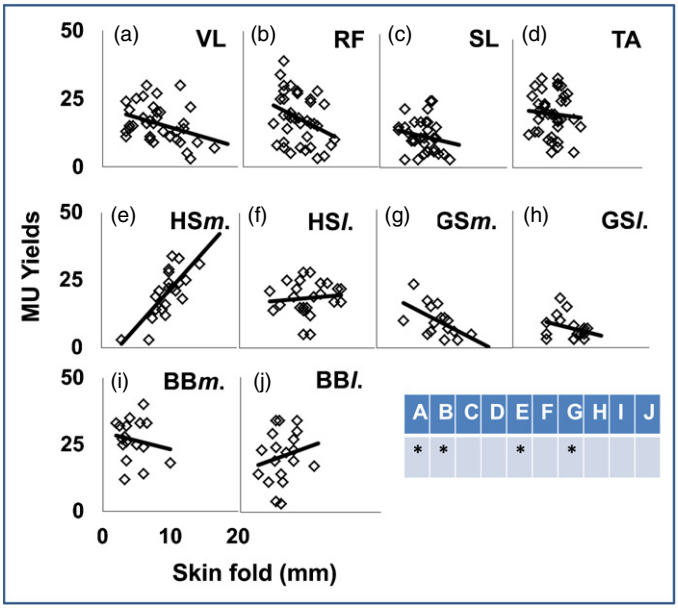

Figure 6. The regressions of the MU yields against the skinfold thickness. Each panel contains the data from one of the tested muscles. The table indicates with an asterisk (*) the significant correlations. The medial HS muscle presents anomalous trend that was also significant. See table 3 for statistics.

portions of the muscle; typically the latter. These sites differ from preferred sensor locations recommended for conventional kinesiology sEMG studies using bar electrodes where the intent is to acquire global muscle activity. For those applications, the preferred sensor site is in the center of the muscle belly (De Luca 1997). The present study nonetheless confirms that reasonable MU yields can be obtained from multiple sites on the muscle belly for sEMG MU studies. However, certain sites are recommended for the richer MU yields as reported here.

The finding that muscles have localized regions that provide greater MU yields is likely related to alterations in the sEMG signal resulting from the tissue inhomogeneity across the muscle surface, as well as the quality of electrical contact between the pins (electrodes) of the sensor and the skin. As expected, there exists a direct relationship between the MU yield and the SNR of the sEMG signal. When more of the sEMG signal is distinguishable above the noise level, the decomposition algorithm is more able to identify and distinguish the action potentials in the signal. There appears to be a minimum SNR level of 3 in the collected signal below which the MU yield is either poor or unreliable. An exception seen in figure 4 is the case of the lateral BB muscle whose SNR values are in fact unevenly distributed throughout its range.

One likely source of decreasing SNR is the presence of fatty tissue between the skin and the surface of the muscle. The increased space acts as a low-pass filter which decreases the amplitude of the sEMG signal originating in the muscle. As expected, the association between SNR and skinfold was found to be negative, reaching statistical significance for most muscles. The negative relationship in the lateral GS was not significant likely due to the low range of skinfold values in this muscle. The HS muscle is unique in the group of muscles tested in that it has a tight layer of fascia overlying the muscle. The tautness of the fascia renders the measurement of the skinfold difficult and unreliable. It is likely that this is the reason why the

relationship between the SNR and the skinfold in the medial HS did not reach significance. Similarly, the relationship between MU yields and skinfold was generally found to be negative for all the muscles tested, with the sole exception of the medial HS muscle, as shown in figure 6. In the medial and lateral BB, SL, TA, lateral HS and lateral GS muscles the range of skinfold value was low compared to the other muscles. Consequently, their R^2 values were low, ranging from 0.01 to 0.07, and the regressions were not significant.

Although the data indicate the presence of preferred sensor sites on the muscle that were associated with lower skinfold thicknesses, the relationship is not completely consistent and not statistically robust. It appears that there are other factors that influence the MU yield. The dominant among them is likely to be the muscle innervation zone. It is known that the region in the vicinity of the innervation zones produces sEMG signals with lower amplitudes, hence lower SNR (Basmajian and De Luca 1985, Rainoldi *et al* 2004) due to the cancellation of the action potentials traveling in opposite directions. It has also been shown by Roy *et al* (1986) that the frequency spectrum of the sEMG signal detected near the innervation zone has more higher frequency components. These are due to the more complex action potentials that are present in this region. They present a greater challenge to the decomposition algorithm, resulting in fewer units being identified. It was beyond the scope of this study to locate the innervation zones on each of the tested muscles. We focused on identifying easy to locate landmarks that could be used to guide the fruitful placement of the sensor for collecting data that would provide the greatest MU yield from the decomposition algorithm. In summary, almost all locations on the surface of a muscle provide sEMG signals that may be decomposed to yield the firing instances and shapes of several MUs. However, muscles have preferred sites that provide richer MU yields. They are generally located between the center of the muscle belly and the tendinous areas of the muscle. These sites are associated with regions where the easily measurable skinfolds have the least thickness. Additionally, we recommend a minimal SNR of 3 for reliable MU yields.

Acknowledgments

This work was supported in part by grant HD050111 from NCMRR/NICHD/NIH. We thank all the subjects who patiently collaborated in the experiments. We also thank senior project students Allie Paquette and Megan Fessenden for their assistance in data collection and data processing.

References

Adam A and De Luca C J 2003 Recruitment order of motor units in human vastus lateralis muscle is maintained during fatiguing contractions *J. Neurophysiol.* **90** 2919–27

Basmajian J and De Luca C J 1985 Apparatus, Detection and Recording Techniques *Muscles Alive* 5th edn (Baltimore, MD: Williams & Wilkins) pp 60–4

Cole T J 1991 Weight-stature indices to measure underweight, overweight and obesity *Anthropometric Assessment of Nutritional Status* (New York: Wiley-Liss) pp 83–111

De Luca C J 1997 The use of surface electromyography in biomechanics *J. Appl. Biomech.* **13** 135–63

De Luca C J, Adam A, Wotiz R, Gilmore D and Nawab S H 2006 Decomposition of surface EMG signals *J. Neurophysiol.* **96** 1646–57

De Luca C J and Hostage E 2010 Relationship between firing rate and recruitment threshold of motoneurons in voluntary isometric contractions *J. Neurophysiol.* **104** 1034–46

Edwards D A W 1954 Design and accuracy of calipers for measuring subcutaneous tissue thickness *Br. J. Nutrition* **9** 133–43

Gazzoni M, Farina D and Merletti R 2004 A new method for the extraction and classification of single motor unit action potentials from surface EMG signals *J. Neurosci. Methods* **136** 165–77

Holobar A, Farina D, Gazzoni M, Merletti R and Zazula D 2009 Estimating motor unit discharge patterns from high-density surface elctromyogram *J. Neurophysiol.* **102** 1890–901

LeFever R S and De Luca C J 1982 A procedure for decomposing the myoelectric signal into its constituent action potentials: part I—technique, theory and implementation *IEEE Trans. Biomed. Eng.* **29** 149–57

Merletti R, Botter A, Troiano A, Merlo E and Minetto M A 2009 Technology and instrumentation for detection and conditioning of the surface electromyographic signal: state of the art *Clin. Biomech.* **24** 122–34

Nawab S H, Chang S and De Luca C J 2010 High-yield decomposition of surface EMG signals *Clin. Neurophysiol.* **121** 1602–15

Nawab S H, Wotiz R P and De Luca C J 2008 Decomposition of indwelling EMG signals *J. Appl. Physiol.* **105** 700–10

Rainoldi A, Melchiorri G and Caruso I 2004 A method for positioning electrodes during surface EMG recordings in lower limb muscles *J. Neurosci. Methods* **134** 37–43

Roy S H, De Luca C J and Schneider J 1986 Effects of electrode site on myoelectric conduction velocity and median frequency estimates *J. Appl. Physiol.* **61** 1510–7